Growth arrest in the active rare biosphere

Bela Hausmann [1,2], Claus Pelikan [1], Thomas Rattei [3], Alexander Loy [1*], and Michael Pester [2,4*]

[1] University of Vienna, Research Network Chemistry meets Microbiology, Department of Microbiology and Ecosystem Science, Division of Microbial Ecology, Vienna, Austria

[2] University of Konstanz, Department of Biology, Konstanz, Germany

[3] University of Vienna, Research Network Chemistry meets Microbiology, Department of Microbiology and Ecosystem Science, Division of Computational Systems Biology, Vienna, Austria

[4] Leibniz Institute DSMZ, Braunschweig, Germany

* Correspondence: Alexander Loy, University of Vienna, Research Network Chemistry meets Microbiology, Department of Microbiology and Ecosystem Science, Division of Microbial Ecology, Althanstraße 14, 1090 Vienna, Austria. Phone: +43 1 4277 76605. Fax: +43 1 4277 876605. E-mail: loy@microbial-ecology.net; and Michael Pester, Leibniz Institute DSMZ, Inhoffenstraße 7B, 38124 Braunschweig, Germany. Phone: +49 531 2616 237. Fax: +49 531 2616 418. E-mail: michael.pester@dsmz.de.

Significance

The microbial rare biosphere represents the largest pool of biodiversity on Earth and constitutes, in sum of all its members, a considerable part of a habitat's biomass. Dormancy or starvation are typically used to explain a low-abundance state. We show that low-abundance microorganisms can be highly metabolically active while being growth-arrested over prolonged time periods. We show that this is true for microbial keystone species, such as a cosmopolitan but low-abundance sulfate reducer in wetlands that is involved in counterbalancing greenhouse gas emission. Our results challenge the central dogmas "metabolic activity translates directly into growth" as well as "low abundance equals little ecosystem impact" and provide an important step forward in understanding rare biosphere members relevant for ecosystem functions.

Abstract

Microbial diversity in the environment is mainly concealed within the rare biosphere, which is arbitrarily defined as all species with <0.1% relative abundance. While dormancy explains a low-abundance state very well, the cellular mechanisms leading to rare but active microorganisms are not clear. We used environmental systems biology to genomically and metabolically characterize a cosmopolitan sulfate reducer that is of low abundance but highly active in peat soil, where it contributes to counterbalance methane emissions. We obtained a 98%-complete genome of this low-abundance species, *Candidatus Desulfosporosinus infrequens*, by metagenomics. To test for environmentally relevant metabolic activity of *Ca. D. infrequens*, anoxic peat soil microcosms were incubated under diverse *in situ*-like conditions for 36 days and analyzed by metatranscriptomics. Compared to the no-substrate control, transcriptional activity of *Ca. D. infrequens* increased 56- to 188-fold in incubations with sulfate and acetate, propionate, lactate, or butyrate, revealing a versatile substrate use. Cellular activation was due to a significant overexpression of genes encoding ribosomal proteins, dissimilatory sulfate reduction, and carbon-degradation pathways, but not of genes encoding DNA or cell replication. We show for the first time that a rare biosphere member transcribes metabolic pathways relevant for carbon and sulfur cycling over prolonged time periods while being growth-arrested in its lag phase.

Keywords

rare biosphere | growth arrest | keystone species | lag phase | sulfur cycle | systems biology

Author contributions

B.H., A.L., and M.P. designed research; B.H. performed research; T.R. contributed computational resources; B.H., C.P., A.L., and M.P. analyzed data; B.H., A.L., and M.P. wrote the paper.

Introduction

The vast majority of microbial diversity worldwide is represented by the rare biosphere (Sogin *et al.*, 2006; Pedrós-Alió, 2012; Lynch and Neufeld, 2015; Jousset *et al.*, 2017). This entity of microorganisms consists of all microbial species that have an arbitrarily defined relative population size of <0.1% in a given habitat at a given time (Sogin *et al.*, 2006; Pedrós-Alió, 2012; Lynch and Neufeld, 2015; Jousset *et al.*, 2017). The rare biosphere is opposed by a much smaller number of moderately abundant or very abundant microbial species (≥0.1% and ≥1.0% relative abundance, respectively, Hausmann *et al.*, 2016), which are thought to be responsible for the major carbon and energy flow through a habitat as based on their cumulative biomass. However, there is accumulating experimental evidence that the rare biosphere is not just a so-called “seed bank” of microorganisms that are waiting to become active and numerically dominant upon environmental change (Müller *et al.*, 2014; Lynch and Neufeld, 2015), but also harbors metabolically active microorganisms with important ecosystem functions (Jousset *et al.*, 2017).

First hints for metabolically active rare biosphere members were evident from seasonal patterns of marine bacterioplankton species. Here, many taxa that displayed recurring annual abundance changes were of low abundance and even during their bloom periods never reached numerically abundant population sizes (Campbell *et al.*, 2011; Hugoni *et al.*, 2013; Alonso-Sáez *et al.*, 2015). In soil environments, removal of low-abundance species by dilution-to-extinction had a positive effect on intruding species, suggesting that active low-abundance species pre-occupy ecological niches and thus slow down invasion (van Elsas *et al.*, 2012; Vivant *et al.*, 2013; Mallon *et al.*, 2015). Soil microorganisms of low relative abundance were also shown to play a role in community-wide species interactions, e.g, by being involved in the production of antifungal compounds that protect plants from pathogens (Hol *et al.*, 2015) or by constituting the core of microorganisms that respond to the presence of a particular plant species (Dawson *et al.*, 2017). Other examples include microorganisms with a specialized metabolism that sustain stable low-abundance populations in an ecosystem (Lynch and Neufeld, 2015). For example, N_2-fixing microorganisms in the ocean (Großkopf *et al.*, 2012) or sulfate-reducing microorganisms (SRM) in peatlands (Pester *et al.*, 2010, 2012b; Hausmann *et al.*, 2016) were shown to fulfill such gatekeeper functions.

A peatland *Desulfosporosinus* species was one of the first examples identified as an active rare biosphere member contributing to an important ecosystem function (Pester *et al.*, 2010). This SRM is involved in the cryptic sulfur cycle of peatlands (Pester *et al.*, 2010; Hausmann *et al.*, 2016), which in turn controls the emission of the greenhouse gas CH_4 from these globally relevant environments (Pester *et al.*, 2012b). Although porewater sulfate concentrations are typically quite low in peatlands (<300 µM, Pester *et al.*, 2012b), these environments are characterized by temporally fluctuating high sulfate reduction rates (up to 1800 nmol cm^{-3} day^{-1}, Pester *et al.*, 2012b). These rates can be in the same range as in sulfate-rich marine surface sediments, where sulfate reduction is one of the major anaerobic carbon degradation pathways (e.g., Jørgensen, 1982; Leloup *et al.*, 2009; Holmkvist *et al.*, 2011a, 2011b). In low-sulfate peatlands, such high sulfate reduction rates can only be maintained by

rapid aerobic or anaerobic re-oxidation of reduced sulfur species back to sulfate (Pester *et al.*, 2012b). Since SRM generally outcompete methanogens and syntrophically associated fermenters (Muyzer and Stams, 2008), they exert an important intrinsic control function on peatland CH_4 production (Gauci *et al.*, 2004, 2005; Gauci and Chapman, 2006). This is important, since natural wetlands, such as peatlands, are estimated to be responsible for 30% of the annual emission of this potent greenhouse gas (Ciais *et al.*, 2013; Kirschke *et al.*, 2013; Saunois *et al.*, 2016).

Little is known about the ecophysiology of metabolically active but low-abundance microorganisms. This lack of knowledge is clearly founded in their low numerical abundance making it inherently difficult to study their metabolic responses or even to retrieve their genomes directly from the environment. In a preceding study, we could show that the low-abundance peatland *Desulfosporosinus* species mentioned above follows an ecological strategy to increase its cellular ribosome content while maintaining a stable population size when exposed to favorable, sulfate-reducing conditions (Hausmann *et al.*, 2016). This was unexpected since metabolic activity in bacteria and archaea is typically immediately followed by growth. Furthermore, this *Desulfosporosinus* species can be found worldwide in a wide range of low-sulfate wetlands including not only peatlands but also permafrost soils and rice paddy fields (Hausmann *et al.*, 2016), which emphasizes its importance as a model organism for active rare biosphere members. In this study, we used an environmental systems biology approach to deepen our understanding of the ecophysiology of this rare biosphere member. In particular, we retrieved its genome directly from a combination of native and incubated peat soil and followed its transcriptional responses in peat soil microcosms, which were exposed to different environmental triggers that mimicked diverse *in situ* conditions.

Results

Recovery of a near complete genome of a rare biosphere member: *Desulfosporosinus* MAG SbF1 represents a novel species

We obtained the population genome of the low-abundance *Desulfosporosinus* species by co-assembly and differential coverage binning of metagenomes obtained from native peat soil and ^{13}C-fractions of a DNA-stable isotope probing experiment (Fig. S1) (Hausmann *et al.*, 2018). The high quality metagenome-assembled genome (MAG) SbF1 had a size of 5.3 Mbp (on 971 scaffolds), a G+C content of 42.6%, a checkM-estimated completeness of 98.0%, a potential residual contamination of 3.9%, and 10% strain heterogeneity. Besides 16S and 23S rRNA genes, SbF1 carried 6440 protein-coding genes (CDS), five 5S rRNA gene copies, 59 tRNAs, and 37 other ncRNAs, making a total of 6543 predicted genomic features. Scaffolds encoding rRNA genes had a higher coverage compared to the average coverage of all scaffolds (Fig. S1), indicating multiple *rrn* operon copies, as is known from other *Desulfosporosinus* genomes. The 16S rRNA gene was 100% identical to *Desulfosporosinus* OTU0051, which was previously shown to correlate strongest among all recognized SRM to sulfate turnover in microcosms of the analyzed peat soil (Hausmann *et al.*, 2016). The genome size and G+C content was in the same range as observed for genomes of cultured *Desulfosporosinus* species (3.0–5.9 Mbp and 42–44%, respectively; Abicht *et al.*, 2011; Pester *et al.*,

2012a; Abu Laban *et al.*, 2015; Petzsch *et al.*, 2015; Mardanov *et al.*, 2016).

In the 16S rRNA tree, SbF1 formed a well supported clade with *Desulfosporosinus* sp. 44a-T3a (98.3% sequence identity), *Desulfosporosinus* sp. OT (98.8%), and *Desulfosporosinus* sp. 5apy (98.1%). The most similar validly described species was *D. lacus* with a sequence identity of 97.5% (Fig. S2a). Phylogenomics confirmed *Desulfosporosinus* sp. OT as the closest relative (Fig. S2b) with average amino and nucleic acid identities (AAI and ANI) of 77% and 79%, respectively (Fig. S3). The intra-genus AAI variability of *Desulfosporosinus* species was 69–93% (Fig. S3). MAG SbF1 represents a novel species in this genus based on species-level thresholds of 99% for the 16S rRNA gene (Stackebrandt and Ebers, 2006) and 96.5% for ANI (Varghese *et al.*, 2015).

The versatile energy metabolism of the low-abundance *Desulfosporosinus*

Desulfosporosinus MAG SbF1 encoded the complete canonical pathway for dissimilatory sulfate reduction (Fig. 1, Table S1). This encompassed the sulfate adenylyltransferase (Sat), adenylyl-sulfate reductase (AprBA), dissimilatory sulfite reductase (DsrAB), and the sulfide-releasing DsrC, which are sequentially involved in the reduction of sulfate to sulfide. In addition, genes encoding the electron-transferring QmoAB and DsrMKJOP complexes were detected, with their subunit composition being typical for *Desulfosporosinus* species (Abicht *et al.*, 2011; Pester *et al.*, 2012a; Petzsch *et al.*, 2015; Mardanov *et al.*, 2016). Other *dsr* genes included *dsrD*, *dsrN*, and *dsrT* (Rabus *et al.*, 2015), with hitherto unvalidated function, as well as *fdxD*, which encodes a [4Fe4S]-ferredoxin, and a second set of DsrMK-family encoding genes (*dsrM2* and *dsrK2*). SbF1 also encoded the trimeric dissimilatory sulfite reductase AsrABC (anaerobic sulfite reductase) (Huang and Barrett, 1991).

SbF1 carries genes for both complete and incomplete oxidation of propionate and lactate. In addition, the ability to utilize acetate, formate, or H_2 as electron donors was encoded (Fig. 1). All enzymes necessary for propionate oxidation to the central metabolite pyruvate (including those belonging to a partial citric acid cycle) were encoded on two scaffolds (Table S1). For lactate utilization, SbF1 carried three paralogs of glycolate/D-lactate/L-lactate dehydrogenase family genes. However, the substrate specificity of the encoded enzymes could not be inferred from sequence information alone. The transcription of *lutDF* and *lutD_2* was stimulated by the addition of L-lactate (Fig. 1), which indicates that these genes encode functional lactate dehydrogenases (LDH). The third paralog (*glcDF*, Table S1) was not stimulated by lactate. LutDF was organized in an operon with a lactate permease (LutP) and a lactate regulatory gene (*lutR*). LutD_2 was organized in a operon with an electron-transferring flavoprotein (EtfBA_2), which resembled the electron-confurcating LDH/Etf complex in *Acetobacterium woodii* (Weghoff *et al.*, 2015). LDHs have been shown to utilize both L- and D-lactate (e.g., Weghoff *et al.*, 2015; Zhang *et al.*, 2016). However, SbF1 also encoded a lactate racemase (LarA) and a lactate racemase-activating system (LarEBC) for interconversion of both stereoisomers (Desguin *et al.*, 2014).

Pyruvate, the intermediate product in propionate and lactate degradation, can be further oxidized to acetyl-CoA with either one of several pyruvate-ferredoxin oxidoreductases (PfoA) or formate C-

acetyltransferase (PflD). Acetyl-CoA can then be completely oxidized to CO_2 via the Wood–Ljungdahl pathway (Pierce *et al.*, 2008), which is complete in SbF1 (Fig. 1, Table S1) and present in the genomes of all other sequenced *Desulfosporosinus* species (Abicht *et al.*, 2011; Pester *et al.*, 2012a; Petzsch *et al.*, 2015; Mardanov *et al.*, 2016). Alternatively, acetyl-CoA may be incompletely oxidized to acetate via acetyl-phosphate by phosphate acetyltransferase (Pta) and acetate kinase (AckA). Pta and AckA are bidirectional enzymes, opening the possibility that acetate could be degraded via these two enzymes and the downstream Wood–Ljungdahl pathway to CO_2.

Formate and H_2 represented additional potential electron donors for SbF1. Its genome encoded three formate dehydrogenases (FDH). FDH-1 consists of three subunits (*fdhCBA*) while FDH-2 (FdhA_2) and FDH-3 (FdhA-3) are monomeric enzymes. In addition, [NiFe] hydrogenases of group 1 and 4f, as well as [FeFe] hydrogenases of group A (Greening *et al.*, 2016) were encoded. Homologs of genes for butyrate oxidation were missing in SbF1 (Schmidt *et al.*, 2013), which is in contrast to other *Desulfosporosinus* species (e.g., *D. orientis*). Both glycolysis and gluconeogenesis were complete. However, neither a glucokinase or a phosphotransferase system was found (PTS). Coupling of electron transfer to energy conservation could be mediated in SbF1 by a H^+/Na^+-pumping Rnf complex (RnfCDGEAB) (Buckel and Thauer, 2013) and a NADH dehydrogenase (respiratory complex I, NuoABCDEFGHIJKLMN). In addition, the complete gene set for ATP synthase (AtpABCDEFGH) was identified (Fig. 1, Table S1).

Activation of energy metabolism is uncoupled from cell division initiation

We used metatranscriptomics to analyse gene expression changes of *Desulfosporosinus* MAG SbF1 in anoxic peat microcosms, which mimicked diverse *in situ*-like conditions. Total transcriptional activity of *Desulfosporosinus* MAG SbF1 was clearly stimulated by individual additions of acetate, propionate, lactate, and butyrate in combination with sulfate. In these incubations, total mRNA counts of SbF1 increased by 56-, 80-, 62-, and 188-fold as compared to the no-substrate-control, respectively, and constituted between 0.11 ± 0.13% (acetate) and 0.36 ± 0.02% (butyrate) of all transcripts in the respective metatranscriptomes after 36 days (Fig. 2a). This substrate-specific activity was mirrored in the increased transcription of genes encoding ribosomal proteins as general activity markers (Fig. 2b) and of all dissimilatory sulfate reduction genes, except the alternative pathway via *asrABC* (Fig. 3). For example, Spearman's rank correlation coefficients of *dsrA* and *dsrB* transcripts as compared to total mRNA counts were 0.91 and 0.90, respectively (FDR-adjusted *p*-value < 0.001). Other enzyme complexes involved in the central metabolism of SbF1 such as the ATP synthase, the NADH dehydrogenase (complex I), and ribosomal proteins followed the same transcriptional pattern (Fig. 3) with an average Spearman's rank correlation coefficients of 0.79 ± 0.07 (n = 72, FDR-adjusted *p*-value < 0.05) to total mRNA counts. Interestingly, transcription of genes encoding proteins involved in general stress response were stimulated as well. In particular, genes encoding the universal stress promotor UspA and the GroSL chaperonin showed an increased transcription (Fig. 3) with an average Spearman's rank correlation coefficients of 0.76 ± 0.06 (n = 3, FDR-adjusted *p*-value < 0.05) to total mRNA counts.

In addition, we screened the COG categories D, L, and M for indicator genes that encode functions in cell division (e.g., *ftsZ* or *minE*), DNA replication (e.g., *gyrBA*, *dnaC*, and *dnaG*) and cell envelope biogenesis (e.g., *murABCDEFGI*), respectively, and followed their expression patterns. Genes that unambiguously encoded such functions (Table S1) showed either no or only barely detectable but insignificant (FDR-adjusted *p*-value > 0.05) increases in transcripts under these conditions (Fig. 2b, detailed in Fig. S4). Extension of this analysis to all genes belonging to COG D (n = 73), L (n = 280), and M (n = 215), which included also genes with ambiguous classification or unknown function, revealed that also here 96%, 99%, and 99%, respectively, were not significantly overexpressed under acetate, propionate, lactate, and butyrate in combination with sulfate (Table S1, Table S3). Here, the average Spearman's rank correlation coefficients to total mRNA counts was only 0.45 ± 0.13 (FDR-adjusted *p*-value < 0.05, Table S1).

We also analysed genes reported to be upregulated immediately after phage infection, as a potential ecological driver that controls bacterial population size. Respective genes in *Bacillus subtilis* encode, e.g., functions in DNA and protein metabolism and include the ribonucleoside-diphosphate reductase (*nrdEF*), aspartyl/glutamyl-tRNA amidotransferase (*gatCAB*), and the proteolytic subunit of ATP-dependent Clp protease (*clpP*) (Mojardín and Salas, 2016). However, homologs in SbF1 were not significantly overexpressed (FDR-adjusted *p*-value > 0.05), which was reflected in an average Spearman's rank correlation coefficient of 0.63 ± 0.08 (n = 5, FDR-adjusted *p*-value < 0.05) to total mRNA counts. The same was true when screening for active sporulation of a *Desulfosporosinus* subpopulation as an alternative explanation for a low population size. The identified sporulation genes (*spo0A–spoVT*) did not show any significant increase in transcript numbers as well, with the only exception of *spoIIIAD*. This stage III sporulation gene was significantly more abundant when stimulated with propionate and sulfate, however did not correlate to total mRNA levels (Table S1). Again, genes involved in sporulation had a low average Spearman's rank correlation coefficient of 0.44 ± 0.13 (n = 22, FDR-adjusted *p*-value < 0.05) to total mRNA counts.

The individual incubation regimes additionally triggered transcriptional activation of the respective substrate degradation pathways of *Desulfosporosinus* MAG SbF1. For example, all genes necessary for the conversion of propionate to pyruvate were overexpressed only upon addition of propionate and sulfate but not in any other incubation type. The same was true for lactate degradation, where genes encoding the lactate permease, lactate racemase and two of the detected lactate dehydrogenases were overexpressed upon addition of both lactate and sulfate, but not in incubations with lactate only (Fig. 3). Although genes encoding phosphotransacetylase and acetate kinase were overexpressed under lactate and propionate, the complete Wood–Ljungdahl pathway was overexpressed as well, which indicates that at least part of these substrates were completely degraded to CO_2 rather than to acetate and CO_2. This conclusion was supported by the overexpression of the Wood–Ljungdahl pathway in incubations amended with acetate and sulfate. Interestingly, the Wood–Ljungdahl pathway was also overexpressed upon addition of butyrate and sulfate. Under such conditions, *Desulfosporosinus* MAG SbF1 apparently relies on a synthrophic lifestyle based on acetate uptake as it lacked the capability for butyrate oxidation; albeit failed

recovery of the butyrate degradation pathway during binning cannot be excluded.

Discussion

Current knowledge on the mechanisms that interconnect energy metabolism, gene expression, cell division, and population growth of microorganisms are mainly based on pure cultures that can be easily maintained in the laboratory. Here, the typical lifecycle of a metabolically active microorganisms would go through an activating lag phase, an exponential growth phase, and a stationary phase upon limitation of substrate, nutrient, or space. Under ideal conditions, a single Escherichia coli cell would grow to a population with the mass of the Earth within 2 days. Clearly, this does not occur, but the discrepancy between potential and actual growth underscores that microorganisms spend the vast majority of their time not dividing (Bergkessel *et al.*, 2016). A large fraction of these microorganisms is part of the rare biosphere. For example, in the studied peatland, the sum of all low-abundance species made up approximately 12% of the total bacterial and archaeal 16S rRNA genes (Hausmann *et al.*, 2016). In other soils, low-abundance *Alphaproteobacteria* and *Bacteroidetes* alone constituted in sum 10% and 9% of the total bacterial population, respectively, while all low-abundance populations summed up to 37% of all bacteria (Dawson *et al.*, 2017). Upon strong environmental change, low-abundance microorganisms often grow to numerically abundant populations and replace dominant species as observed for microbial community changes after an oil spill (Teira *et al.*, 2007; Newton *et al.*, 2013) or in the response of soil microorganisms towards the presence of plants (Dawson *et al.*, 2017). However, subtle environmental changes (Hausmann *et al.*, 2016) or recurring seasonal shifts (Campbell *et al.*, 2011; Vergin *et al.*, 2013; Alonso-Sáez *et al.*, 2015) often lead to rather small shifts in low-abundance populations without rare biosphere members becoming numerically dominant.

The low-abundance *Desulfosporosinus* MAG SbF1 represents an interesting case of the latter response type. When exposed to favorable, sulfate-reducing conditions in peat soil microcosms, it did not increase its population size but drastically increased its cellular ribosome content by one order of magnitude to 57,000–84,000 16S rRNA molecules per cell (Hausmann *et al.*, 2016). Throughout the incubation period of 50 days, it correlated best in its 16S rRNA response to sulfate turnover among all identified SRM (Hausmann *et al.*, 2016). In this study, we expanded upon this observation by genome-centric metatranscriptomics to test whether the increase in cellular ribosome content is indeed translated into increased transcriptional and, as a consequence, metabolic activity of *Desulfosporosinus* MAG SbF1. As expected, increases in cellular 16S rRNA content clearly corresponded to increased transcription of genes coding for ribosomal proteins (Fig. 2b; Hausmann *et al.*, 2016). This cellular ribosome increase under sulfate-reducing conditions was correlated to an increase in total mRNA counts (Fig. 2). This is the first time that changes in population-wide 16S rRNA levels are proven to be directly linked to transcriptional activity for a rare biosphere member.

Analyzing the transcriptional response of a rare biosphere member under *in situ*-like conditions opens the unique opportunity to gain insights into its ecophysiology. *Desulfosporosinus* MAG SbF1

clearly overexpressed its sulfate reduction pathway under sulfate amendment when supplied with either acetate, lactate, propionate, or butyrate as compared to the no-substrate and the methanogenic controls (Fig. 3). Detailed analysis of the transcribed carbon degradation pathways showed that *Desulfosporosinus* MAG SbF1 is able to oxidize propionate, lactate, and acetate completely to CO_2. Under butyrate-amended conditions it presumably relied on syntrophic oxidation of acetate supplied by a primary butyrate oxidizer. This shows that *Desulfosporosinus* MAG SbF1 is capable of utilizing diverse substrates that represent the most important carbon degradation intermediates measured in peatlands (Schmalenberger *et al.*, 2007; Küsel *et al.*, 2008). Such a generalist lifestyle is of clear advantage in peat soil given the highly variable nutrient and redox conditions (Schmalenberger *et al.*, 2007; Küsel *et al.*, 2008). These fluctuations are caused by the periodically changing water table that steadily shifts the oxic–anoxic interface (Knorr *et al.*, 2009; Reiche *et al.*, 2009). In addition, the complex flow paths of water create distinct spatial and temporal patterns (hot spots and hot moments) of various biogeochemical parameters, to which peat microorganisms have to adapt (Jacks and Norrström, 2004; Knorr *et al.*, 2009; Knorr and Blodau, 2009; Frei *et al.*, 2012).

The question remains, which mechanisms are at work that keep the *Desulfosporosinus* MAG SbF1 population in a stable low-abundance state? Population sizes can be kept low by actively restricting growth. Alternatively, ongoing growth could be hidden by continuous predation, viral lysis, or active sporulation of a major subpopulation. To answer this question, we analysed expression patterns of growth-specific genes. Compared to the strong overexpression of metabolic or ribosomal protein genes, transcription of genes essential for DNA replication, cell division, and cell envelope biogenesis did not increase or only marginally (Fig. 2b, Fig. S4). Genes encoding DNA replication or cell division typically show a largely invariable transcription in the exponential and stationary phase (e.g., Sumby *et al.*, 2012; Brudal *et al.*, 2013; Sihto *et al.*, 2014). However, there is experimental evidence that in the lag phase transcription of growth-specific genes is not stable but increases due to the overall activation of cellular processes (Rolfe *et al.*, 2012). In this context, the lack of an increasing transcription of growth-specific genes would clearly indicate a state of no growth rather than an actively dividing population that is kept stable by an equally high growth and mortality or sporulation rate. This conclusion is further corroborated by the lack of overexpressed sporulation genes or genes upregulated directly after phage attack. Nevertheless, the ATP generated by the induced energy metabolism has to be utilized somehow. This could be mediated by the production of storage compounds or by counterbalancing environmental stress. We found no indication for the former scenario but observed overexpression of the universal stress promotor UspA, which is one of the most abundant proteins in growth-arrested cells (Kvint *et al.*, 2003), and the chaperonin GroSL, which was linked previously to stress response such as low pH (Silva *et al.*, 2005). Since the pH in the analyzed peat soil incubations varied between 4.1–5.0 (Hausmann *et al.*, 2016), coping with a low pH would be the most likely reason that deviates ATP away from growth towards stress response. Based on the integrated findings of our previous study (stable population over 50 days as based on 16S rRNA gene counts; Hausmann *et al.*, 2016), and this study (no activation of the DNA replication and cell division machinery within 36 days), we propose that *Desulfosporosinus* MAG SbF1

was growth-arrested in the lag phase over a period of at least 50 days while being a metabolically active rare biosphere member. This finding shows that growth arrest is not restricted to starving or otherwise limited microorganisms that persist in the environment (Bergkessel *et al.*, 2016) but can also occur in metabolically highly active microorganisms.

Our results are important in the context of the increasing awareness that the microbial rare biosphere is not only the largest pool of biodiversity on Earth (Sogin *et al.*, 2006; Pedrós-Alió, 2012; Lynch and Neufeld, 2015; Jousset *et al.*, 2017) but in sum of all its low-abundance members constitutes also a large part of the biomass in a given habitat (e.g., Hausmann *et al.*, 2016; Dawson *et al.*, 2017). Understanding the mechanisms governing this low-abundance prevalence and its direct impact on ecosystem functions and biogeochemical cycling is thus of utmost importance. *Desulfosporosinus* MAG SbF1 has been repeatedly shown to be involved in cryptic sulfur cycling in peatlands (Pester *et al.*, 2010; Hausmann *et al.*, 2016) — a process that counterbalances the emission of the greenhouse gas methane due to the competitive advantage of SRM as compared to microorganisms involved in the methanogenic degradation pathways (Muyzer and Stams, 2008). This species can be found worldwide in low-sulfate environments impacted by cryptic sulfur cycling including not only peatlands but also permafrost soils, rice paddies, and other wetland types (Hausmann *et al.*, 2016). Here, we provided proof that *Desulfosporosinus* MAG SbF1 is indeed involved in the degradation of important anaerobic carbon degradation intermediates in peatlands while sustaining a low-abundance population. It has a generalist lifestyle in respect to the usable carbon sources, re-emphasizing its importance in the carbon and sulfur cycle of peatlands. Our results provide an important step forward in understanding the microbial ecology of biogeochemically relevant microorganisms and show that low-abundance keystone species can be studied “in the wild” using modern environmental systems biology approaches.

Proposal of *Candidatus Desulfosporosinus infrequens*

Based on its phylogenetic placement and novel ecophysiological behaviour, we propose that *Desulfosporosinus* MAG SbF1 represents a novel species with the provisional name *Candidatus Desulfosporosinus infrequens* sp. nov. (in.fre’quens. L. adj. *infrequens*, rare, referring to its low relative abundance). Based on its genome-derived metabolic potential and support from metatranscriptomics, *Ca. D. infrequens* is capable of complete oxidation of acetate, propionate and lactate with sulfate as the electron acceptor, with further potential for oxidation of molecular hydrogen (Fig. 1).

Materials and Methods

Genome assembly, binning, and phylogenetic inference

Sampling of peat soil from the acidic peatland Schlöppnerbrunnen II (Germany), DNA-stable isotope probing (DNA-SIP), total nucleic acids extraction, metagenome sequencing and assembly, and coverage-based binning was described previously (Pester *et al.*, 2010, Hausmann *et al.* (2016);

Hausmann *et al.*, 2018). In brief, DNA from native peat soil (10–20 cm depth) and DNA pooled from 16 ^{13}C-enriched fractions (density 1.715–1.726 g mL^{-1}) of a previous DNA-SIP experiment with soil from the same site (Pester *et al.*, 2010) was sequenced using the Illumina HiSeq 2000 system. DNA-SIP was performed after a 73-day incubation (again 10–20 cm depth) that was periodically amended with small dosages of sulfate and first a mixture of unlabeled formate, acetate, propionate, and lactate for two weeks and thereafter a mixture of ^{13}C-labeled formate, acetate, propionate, and lactate (all in the lower µM-range) (Pester *et al.*, 2010). Raw reads were quality filtered, trimmed, and co-assembled into one metagenomic assembly using the CLC Genomics Workbench 5.5.1 (CLC Bio). Differential coverage binning was applied to extract the *Desulfosporosinus* metagenome-assembled genome (MAG) (Albertsen *et al.*, 2013). A side effect of sequencing a DNA-SIP sample is an apparent G+C content skew, which was normalized arbitrarily to improve binning using the following formula (Herbold *et al.*, 2017; Hausmann *et al.*, 2018):

$$\frac{Coverage}{G+C\ content^{9}} \times 10^{15}$$

Scaffolds encoding the 16S and 23S rRNA genes were successfully identified using paired-end linkage data (Albertsen *et al.*, 2013). Completeness, contamination, and strain heterogeneity was estimated using CheckM 1.0.6 (Parks *et al.*, 2015).

Phylogenomic analysis of the *Desulfosporosinus* MAG was based on a concatenated set of 34 phylogenetically informative marker genes as defined by Parks *et al.* (2015) and the Bayesian phylogeny inference method PhyloBayes using the CAT-GTR model (Lartillot *et al.*, 2009). 16S rRNA gene-based phylogeny was inferred using the ARB SILVA database r126 as a reference (Quast *et al.*, 2013), the SINA aligner (Pruesse *et al.*, 2012), and the substitution model testing and maximum likelihood treeing method IQ-TREE (Trifinopoulos *et al.*, 2016). Pairwise 16S rRNA gene sequence identities were calculated with T-Coffee 11 (Notredame *et al.*, 2000). Pairwise average nucleic and amino acid identities (ANI, AAI, Varghese *et al.*, 2015) between protein-coding genes of the *Desulfosporosinus* MAG and reference genomes were calculated as described previously (Hausmann *et al.*, 2018)

Genome annotation

The genome was annotated using the MicroScope annotation platform (Vallenet *et al.*, 2017). Annotation refinement for selected genes was done as follows: proteins with an amino acid identity ≥40% (over ≥80% of the sequence) to a Swiss-Prot entry (The UniProt Consortium, 2017), curated MaGe annotation (Vallenet *et al.*, 2017), or protein described in the literature were annotated as true homologos of known proteins. The same was true, if classification according to InterPro families (Mitchell *et al.*, 2015; Jones *et al.*, 2014), TIGRFAMs (Haft *et al.*, 2003), and/or FIGfams (Overbeek *et al.*, 2014) led to an unambiguous annotation. Proteins with an amino acid identity ≥25% (over ≥80% of the sequence) to a Swiss-Prot or TrEMBL (The UniProt Consortium, 2017) entry were annotated as

putative homologs of the respective database entries. In addition, classification according to COG (Galperin *et al.*, 2015) or InterPro superfamilies, domains, or binding sites were used to call putative homologs in cases of an unambiguous annotation. Membership to syntenic regions (operons) was considered as additional support to call true or putative homologs.

Metatranscriptomics from single-substrate incubations

We analysed total RNA from anoxic peat soil slurry microcosms that were described previously (Hausmann *et al.*, 2016, 2018). In brief, anoxic microcosms were incubated at 14 °C in the dark for 50 days and regularly amended with either low amounts of sulfate (76–387 µM final concentrations) or incubated without an external electron acceptor. Formate, acetate, propionate, lactate, butyrate (<200 µM), or no external electron donor was added to biological triplicates each. RNA was extracted from the native soil, and after 8 and 36 days of incubations, followed by sequencing with the Illumina HiSeq 2000/2500 system. Raw reads were quality-filtered as described previously (Hausmann *et al.*, 2018) and mapped to the combined metagenomic assembly using Bowtie 2 (Langmead and Salzberg, 2012). Counting of mapped reads to protein-coding genes (CDS) was performed with featureCounts 1.5.0 (Liao *et al.*, 2014). We used an unsupervised approach to identify CDS stimulated by sulfate and the different substrates regimes. First, we applied the DESeq2 R package (Love *et al.*, 2014; R Core Team, 2017) to identify differentially expressed CDS. Treatments without external sulfate added and samples after 8 days of incubations had too little transcript counts to be used for a statistical approach. Therefore, we limited our analysis to pairwise comparison of sulfate-stimulated microcosms after 36 days of incubations. We compared each substrate regime to the no-substrate controls and each other. The set of all significantly differentially expressed CDS (FDR-adjusted p-value < 0.05) were further clustered into response groups. For clustering, we calculated pairwise Pearson's correlation coefficients (r) of variance stabilized counts (cor function in R), transformed this into distances ($1-r$), followed by hierarchical clustering (hclust function in R). Variance stabilisation was performed using the rlog function of the DESeq2 package.

Sequence data availability

The MAG SbF1 is available at MicroScope (https://www.genoscope.cns.fr/agc/microscope/) and is also deposited under the ENA accession number OMOF01000000. Metagenome and -transcriptomic data is available at the Joint Genome Institute (https://genome.jgi.doe.gov/) and is also deposited under the NCBI accession numbers PRJNA412436 and PRJNA412438, respectively.

Acknowledgements

We are grateful to Norbert Bittner, Mads Albertsen, Craig Herbold, Stephan Köstlbacher, and Florian Goldenberg for technical support. We further thank Bernhard Schink for help in naming *Ca. D. infrequens* and Johannes Wittmann and Silvia Bulgheresi for helpful expert opinions. We acknowledge the LABGeM (CEA/IG/Genoscope & CNRS UMR8030) and the France Génomique National infrastructure (funded as part of Investissement d'avenir program managed by Agence

Nationale pour la Recherche, contract ANR-10-INBS-09) for support with the MicroScope annotation platform. The work conducted by the Joint Genome Institute was supported by the Office of Science of the U.S. Department of Energy under Contract No. DE-AC02-05CH11231. This research was financially supported by the Austrian Science Fund (FWF, P23117-B17 to MP and AL, P25111-B22 to AL), the U.S. Department of Energy (CSP605 to MP and AL), the German Research Foundation (DFG, PE 2147/1-1 to MP), and the European Union (FP7-People-2013-CIG, Grant No PCIG14-GA-2013-630188 to MP).

References

Abicht HK, Mancini S, Karnachuk OV, Solioz M. (2011). Genome sequence of *Desulfosporosinus* sp. OT, an acidophilic sulfate-reducing bacterium from copper mining waste in Norilsk, Northern Siberia. *J Bacteriol* **193**: 6104–6105.

Abu Laban N, Tan B, Dao A, Foght J. (2015). Draft genome sequence of uncultivated *Desulfosporosinus* sp. strain Tol-M, obtained by stable isotope probing using [$^{13}C_6$]toluene. *Genome Announc* **3**: e01422–14.

Albertsen M, Hugenholtz P, Skarshewski A, Nielsen KL, Tyson GW, Nielsen PH. (2013). Genome sequences of rare, uncultured bacteria obtained by differential coverage binning of multiple metagenomes. *Nat Biotechnol* **31**: 533–538.

Alonso-Sáez L, Díaz-Pérez L, Morán XAG. (2015). The hidden seasonality of the rare biosphere in coastal marine bacterioplankton. *Environ Microbiol* **17**: 3766–3780.

Bergkessel M, Basta DW, Newman DK. (2016). The physiology of growth arrest: uniting molecular and environmental microbiology. *Nat Rev Microbiol* **14**: 549–562.

Brudal E, Winther-Larsen HC, Colquhoun DJ, Duodu S. (2013). Evaluation of reference genes for reverse transcription quantitative PCR analyses of fish-pathogenic *Francisella* strains exposed to different growth conditions. *BMC Res Notes* **6**: 76.

Buckel W, Thauer RK. (2013). Energy conservation via electron bifurcating ferredoxin reduction and proton/Na^+ translocating ferredoxin oxidation. *Biochim Biophys Acta* **1827**: 94–113.

Campbell BJ, Yu L, Heidelberg JF, Kirchman DL. (2011). Activity of abundant and rare bacteria in a coastal ocean. *Proc Natl Acad Sci USA* **108**: 12776–12781.

Ciais P, Sabine C, Bala G, Bopp L, Brovkin V, Canadell J *et al.* (2013). Carbon and Other Biogeochemical Cycles. In: Stocker T, Qin D, Plattner G-K, Tignor M, Allen S, Boschung J *et al.* (eds). *Climate Change 2013 The Physical Science Basis*. Cambridge University Press. https://www.ipcc.ch/report/ar5/wg1/.

Dawson W, Hör J, Egert M, Kleunen M van, Pester M. (2017). A small number of low-abundance bacteria dominate plant species-specific responses during rhizosphere colonization. *Front Microbiol* **8**: 975.

Desguin B, Goffin P, Viaene E, Kleerebezem M, Martin-Diaconescu V, Maroney MJ *et al.* (2014). Lactate racemase is a nickel-dependent enzyme activated by a widespread maturation system. *Nat Commun* **5**: 3615.

Frei S, Knorr K-H, Peiffer S, Fleckenstein JH. (2012). Surface micro-topography causes hot spots of biogeochemical activity in wetland systems: a virtual modeling experiment. *J Geophys Res Biogeosciences* **117**: G00N12.

Galperin MY, Makarova KS, Wolf YI, Koonin EV. (2015). Expanded microbial genome coverage and improved protein family annotation in the COG database. *Nucleic Acids Res* **43**: D261–D269.

Gauci V, Chapman SJ. (2006). Simultaneous inhibition of CH_4 efflux and stimulation of sulphate reduction in peat subject to simulated acid rain. *Soil Biol Biochem* **38**: 3506–3510.

Gauci V, Dise N, Blake S. (2005). Long-term suppression of wetland methane flux following a pulse of simulated acid rain. *Geophys Res Lett* **32**: L12804.

Gauci V, Matthews E, Dise N, Walter B, Koch D, Granberg G *et al.* (2004). Sulfur pollution suppression of the wetland methane source in the 20th and 21st centuries. *Proc Natl Acad Sci USA* **101**: 12583–12587.

Greening C, Biswas A, Carere CR, Jackson CJ, Taylor MC, Stott MB *et al.* (2016). Genomic and metagenomic surveys of hydrogenase distribution indicate H_2 is a widely utilised energy source for microbial growth and survival. *ISME J* **10**: 761–777.

Großkopf T, Mohr W, Baustian T, Schunck H, Gill D, Kuypers MMM *et al.* (2012). Doubling of marine dinitrogen-fixation rates based on direct measurements. *Nature* **488**: 361–364.

Haft DH, Selengut JD, White O. (2003). The TIGRFAMs database of protein families. *Nucleic Acids Res* **31**: 371–373.

Hausmann B, Knorr K-H, Schreck K, Tringe SG, Glavina del Rio T, Loy A *et al.* (2016). Consortia of low-abundance bacteria drive sulfate reduction-dependent degradation of fermentation products in peat soil microcosms. *The ISME Journal* **10**: 2365–2375.

Hausmann B, Pelikan C, Herbold CW, Köstlbacher S, Albertsen M, Eichorst SA *et al.* (2018). Peatland *Acidobacteria* with a dissimilatory sulfur metabolism. *ISME J*. doi:https://doi.org/10.1038/s41396-018-0077-1[10.1038/s41396-018-0077-1].

Herbold CW, Lehtovirta-Morley LE, Jung M-Y, Jehmlich N, Hausmann B, Han P *et al.* (2017). Ammonia-oxidising archaea living at low pH: insights from comparative genomics. *Environ Microbiol* **19**: 4939–4952.

Hol WHG, Garbeva P, Hordijk C, Hundscheid PJ, Gunnewiek PJAK, Van Agtmaal M *et al.* (2015). Non-random species loss in bacterial communities reduces antifungal volatile production. *Ecology* **96**: 2042–2048.

Holmkvist L, Ferdelman TG, Jørgensen BB. (2011a). A cryptic sulfur cycle driven by iron in the methane zone of marine sediment (Aarhus Bay, Denmark). *Geochim Cosmochim Acta* **75**: 3581–3599.

Holmkvist L, Kamyshny A, Vogt C, Vamvakopoulos K, Ferdelman TG, Jørgensen BB. (2011b). Sulfate reduction below the sulfate–methane transition in Black Sea sediments. *Deep Sea Res Part I Oceanogr Res Pap* **58**: 493–504.

Huang CJ, Barrett EL. (1991). Sequence analysis and expression of the *Salmonella typhimurium asr* operon encoding production of hydrogen sulfide from sulfite. *J Bacteriol* **173**: 1544–1553.

Hugoni M, Taib N, Debroas D, Domaizon I, Jouan Dufournel I, Bronner G *et al.* (2013). Structure of the rare archaeal biosphere and seasonal dynamics of active ecotypes in surface coastal waters. *Proc Natl Acad Sci USA* **110**: 6004–6009.

Jacks G, Norrström A-C. (2004). Hydrochemistry and hydrology of forest riparian wetlands. *For Ecol Manage* **196**: 187–197.

Jones P, Binns D, Chang H-Y, Fraser M, Li W, McAnulla C *et al.* (2014). InterProScan 5: genome-scale protein function classification. *Bioinformatics* **30**: 1236–1240.

Jousset A, Bienhold C, Chatzinotas A, Gallien L, Gobet A, Kurm V *et al.* (2017). Where less may be more: how the rare biosphere pulls ecosystems strings. *ISME J* **11**: 853–862.

Jørgensen BB. (1982). Mineralization of organic matter in the sea bed—the role of sulphate reduction. *Nature* **296**: 643–645.

Kirschke S, Bousquet P, Ciais P, Saunois M, Canadell JG, Dlugokencky EJ *et al.* (2013). Three decades of global methane sources and sinks. *Nat Geosci* **6**: 813–823.

Knorr K-H, Blodau C. (2009). Impact of experimental drought and rewetting on redox transformations and methanogenesis in mesocosms of a northern fen soil. *Soil Biol Biochem* **41**: 1187–1198.

Knorr K-H, Lischeid G, Blodau C. (2009). Dynamics of redox processes in a minerotrophic fen exposed to a water table manipulation. *Geoderma* **153**: 379–392.

Küsel K, Blöthe M, Schulz D, Reiche M, Drake HL. (2008). Microbial reduction of iron and porewater biogeochemistry in acidic peatlands. *Biogeosciences* **5**: 1537–1549.

Kvint K, Nachin L, Diez A, Nyström T. (2003). The bacterial universal stress protein: function and regulation. *Curr Opin Microbiol* **6**: 140–145.

Langmead B, Salzberg SL. (2012). Fast gapped-read alignment with Bowtie 2. *Nat Methods* **9**: 357–359.

Lartillot N, Lepage T, Blanquart S. (2009). PhyloBayes 3: a Bayesian software package for phylogenetic reconstruction and molecular dating. *Bioinformatics* **25**: 2286–2288.

Leloup J, Fossing H, Kohls K, Holmkvist L, Borowski C, Jørgensen BB. (2009). Sulfate-reducing bacteria in marine sediment (Aarhus Bay, Denmark): abundance and diversity related to geochemical zonation. *Environ Microbiol* **11**: 1278–1291.

Liao Y, Smyth GK, Shi W. (2014). featureCounts: an efficient general purpose program for assigning sequence reads to genomic features. *Bioinformatics* **30**: 923–930.

Love MI, Huber W, Anders S. (2014). Moderated estimation of fold change and dispersion for RNA-seq data with DESeq2. *Genome Biol* **15**: 550.

Lynch MDJ, Neufeld JD. (2015). Ecology and exploration of the rare biosphere. *Nat Rev Microbiol* **13**: 217–229.

Mallon CA, Poly F, Le Roux X, Marring I, Elsas JD van, Salles JF. (2015). Resource pulses can alleviate the biodiversity-invasion relationship in soil microbial communities. *Ecology* **96**: 915–926.

Mardanov AV, Panova IA, Beletsky AV, Avakyan MR, Kadnikov VV, Antsiferov DV *et al.* (2016). Genomic insights into a new acidophilic, copper-resistant *Desulfosporosinus* isolate from the oxidized tailings area of an abandoned gold mine. *FEMS Microbiol Ecol* **92**: fiw111.

Mitchell A, Chang H-Y, Daugherty L, Fraser M, Hunter S, Lopez R *et al.* (2015). The InterPro protein families database: the classification resource after 15 years. *Nucleic Acids Res* **43**: D213–D221.

Mojardín L, Salas M. (2016). Global transcriptional analysis of virus-host interactions between phage ϕ29 and *Bacillus subtilis*. *J Virol* **90**: 9293–9304.

Muyzer G, Stams AJM. (2008). The ecology and biotechnology of sulphate-reducing bacteria. *Nat Rev Microbiol* **6**: 441–454.

Müller AL, de Rezende JR, Hubert CRJ, Kjeldsen KU, Lagkouvardos I, Berry D *et al.* (2014). Endospores of thermophilic bacteria as tracers of microbial dispersal by ocean currents. *ISME J* **8**: 1153–1165.

Newton RJ, Huse SM, Morrison HG, Peake CS, Sogin ML, McLellan SL. (2013). Shifts in the microbial

community composition of Gulf Coast beaches following beach oiling. Gilbert JA (ed). *PLoS One* **8**: e74265.

Notredame C, Higgins DG, Heringa J. (2000). T-Coffee: a novel method for fast and accurate multiple sequence alignment. *J Mol Biol* **302**: 205–217.

Overbeek R, Olson R, Pusch GD, Olsen GJ, Davis JJ, Disz T *et al.* (2014). The SEED and the Rapid Annotation of microbial genomes using Subsystems Technology (RAST). *Nucleic Acids Res* **42**: D206–D214.

Parks DH, Imelfort M, Skennerton CT, Hugenholtz P, Tyson GW. (2015). CheckM: assessing the quality of microbial genomes recovered from isolates, single cells, and metagenomes. *Genome Res* **25**: 1043–1055.

Pedrós-Alió C. (2012). The rare bacterial biosphere. *Ann Rev Mar Sci* **4**: 449–466.

Pester M, Bittner N, Deevong P, Wagner M, Loy A. (2010). A 'rare biosphere' microorganism contributes to sulfate reduction in a peatland. *ISME J* **4**: 1591–1602.

Pester M, Brambilla E, Alazard D, Rattei T, Weinmaier T, Han J *et al.* (2012a). Complete genome sequences of *Desulfosporosinus orientis* DSM765^T, *Desulfosporosinus youngiae* DSM17734^T, *Desulfosporosinus meridiei* DSM13257^T, and *Desulfosporosinus acidiphilus* DSM22704^T. *J Bacteriol* **194**: 6300–6301.

Pester M, Knorr K-H, Friedrich MW, Wagner M, Loy A. (2012b). Sulfate-reducing microorganisms in wetlands – fameless actors in carbon cycling and climate change. *Front Microbiol* **3**: 72.

Petzsch P, Poehlein A, Johnson DB, Daniel R, Schlömann M, Mühling M. (2015). Genome sequence of the moderately acidophilic sulfate-reducing firmicute *Desulfosporosinus acididurans* (Strain M1^T). *Genome Announc* **3**: e00881–15.

Pierce E, Xie G, Barabote RD, Saunders E, Han CS, Detter JC *et al.* (2008). The complete genome sequence of *Moorella thermoacetica* (f. *Clostridium thermoaceticum*). *Environ Microbiol* **10**: 2550–2573.

Pruesse E, Peplies J, Glöckner FO. (2012). SINA: accurate high-throughput multiple sequence alignment of ribosomal RNA genes. *Bioinformatics* **28**: 1823–1829.

Quast C, Pruesse E, Yilmaz P, Gerken J, Schweer T, Yarza P *et al.* (2013). The SILVA ribosomal RNA gene database project: improved data processing and web-based tools. *Nucleic Acids Res* **41**: D590–D596.

R Core Team. (2017). R: a language and environment for statistical computing. R Foundation for

Statistical Computing: Vienna, Austria. http://www.r-project.org/.

Rabus R, Venceslau SS, Wöhlbrand L, Voordouw G, Wall JD, Pereira IAC. (2015). A post-genomic view of the ecophysiology, catabolism and biotechnological relevance of sulphate-reducing prokaryotes. *Adv Microb Physiol* **66**: 55–321.

Reiche M, Hädrich A, Lischeid G, Küsel K. (2009). Impact of manipulated drought and heavy rainfall events on peat mineralization processes and source-sink functions of an acidic fen. *J Geophys Res Biogeosciences* **114**: G02021.

Rolfe MD, Rice CJ, Lucchini S, Pin C, Thompson A, Cameron ADS *et al.* (2012). Lag phase is a distinct growth phase that prepares bacteria for exponential growth and involves transient metal accumulation. *J Bacteriol* **194**: 686–701.

Saunois M, Bousquet P, Poulter B, Peregon A, Ciais P, Canadell JG *et al.* (2016). The global methane budget 2000–2012. *Earth Syst Sci Data* **8**: 697–751.

Schmalenberger A, Drake HL, Küsel K. (2007). High unique diversity of sulfate-reducing prokaryotes characterized in a depth gradient in an acidic fen. *Environ Microbiol* **9**: 1317–1328.

Schmidt A, Müller N, Schink B, Schleheck D. (2013). A proteomic view at the biochemistry of syntrophic butyrate oxidation in *Syntrophomonas wolfei*. *PLoS One* **8**: e56905.

Sihto H-M, Tasara T, Stephan R, Johler S. (2014). Validation of reference genes for normalization of qPCR mRNA expression levels in *Staphylococcus aureus* exposed to osmotic and lactic acid stress conditions encountered during food production and preservation. *FEMS Microbiol Lett* **356**: 134–140.

Silva J, Carvalho AS, Ferreira R, Vitorino R, Amado F, Domingues P *et al.* (2005). Effect of the pH of growth on the survival of *Lactobacillus delbrueckii* subsp. *bulgaricus* to stress conditions during spray-drying. *J Appl Microbiol* **98**: 775–782.

Sogin ML, Morrison HG, Huber JA, Mark Welch D, Huse SM, Neal PR *et al.* (2006). Microbial diversity in the deep sea and the underexplored 'rare biosphere'. *Proc Natl Acad Sci USA* **103**: 12115–12120.

Stackebrandt E, Ebers J. (2006). Taxonomic parameters revisited: tarnished gold standards. *Microbiol Today* **33**: 152–155.

Sumby KM, Grbin PR, Jiranek V. (2012). Validation of the use of multiple internal control genes, and the application of real-time quantitative PCR, to study esterase gene expression in *Oenococcus oeni*. *Appl Microbiol Biotechnol* **96**: 1039–1047.

Teira E, Lekunberri I, Gasol JM, Nieto-Cid M, Alvarez-Salgado XA, Figueiras FG. (2007). Dynamics of the hydrocarbon-degrading *Cycloclasticus* bacteria during mesocosm-simulated oil spills. *Environ*

Microbiol **9**: 2551–2562.

The UniProt Consortium. (2017). UniProt: the universal protein knowledgebase. *Nucleic Acids Res* **45**: D158–D169.

Trifinopoulos J, Nguyen L-T, von Haeseler A, Minh BQ. (2016). W-IQ-TREE: a fast online phylogenetic tool for maximum likelihood analysis. *Nucleic Acids Res* **44**: W232–W235.

Vallenet D, Calteau A, Cruveiller S, Gachet M, Lajus A, Josso A *et al.* (2017). MicroScope in 2017: an expanding and evolving integrated resource for community expertise of microbial genomes. *Nucleic Acids Res* **45**: D517–D528.

van Elsas JD, Chiurazzi M, Mallon CA, Elhottova D, Kristufek V, Salles JF. (2012). Microbial diversity determines the invasion of soil by a bacterial pathogen. *Proc Natl Acad Sci USA* **109**: 1159–1164.

Varghese NJ, Mukherjee S, Ivanova N, Konstantinidis KT, Mavrommatis K, Kyrpides NC *et al.* (2015). Microbial species delineation using whole genome sequences. *Nucleic Acids Res* **43**: 6761–6771.

Vergin K, Done B, Carlson C, Giovannoni S. (2013). Spatiotemporal distributions of rare bacterioplankton populations indicate adaptive strategies in the oligotrophic ocean. *Aquat Microb Ecol* **71**: 1–13.

Vivant A-L, Garmyn D, Maron P-A, Nowak V, Piveteau P. (2013). Microbial diversity and structure are drivers of the biological barrier effect against Listeria monocytogenes in soil. *PLoS One* **8**: e76991.

Weghoff MC, Bertsch J, Müller V. (2015). A novel mode of lactate metabolism in strictly anaerobic bacteria. *Environ Microbiol* **17**: 670–677.

Zhang Y, Jiang T, Sheng B, Long Y, Gao C, Ma C *et al.* (2016). Coexistence of two D-lactate-utilizing systems in *Pseudomonas putida* KT2440. *Environ Microbiol Rep* **8**: 699–707.

Figures

Fig. 1

Metabolic model of *Desulfosporosinus* MAG SbF1. Gene expression stimulated by specific substrates in combination with sulfate is indicated by coloured points. Paralogous genes are indicated by an underscore followed by a number. Plus signs indicates proposed protein complexes. Details for all genes are in given in Table S1 and transcription patterns are shown in Fig. 3. For the citric acid cycle and anaplerotic reactions, carriers of reducing equivalents and further by-products are not shown. The following abbreviations were used. X: unknown reducing equivalents, e.g., NAD^+ or ferredoxin. WL: Wood–Ljungdahl pathway consisting of enzymes encoded by the *acs* operon, MetF, FolD, FchA, and Fhs. TCA: citric acid cycle. FDH: formate dehydrogenase. Hase: hydrogenase. NDH-1: NADH dehydrogenase 1. LDH: lactate dehydrogenase.

Fig. 2

Time-resolved transcriptional changes of *Desulfosporosinus* MAG SbF1 in anoxic peat soil microcosms under various *in situ*-like conditions. (a) Total mRNA of all CDS and (b) selected genes encoding the sulfate-reduction pathway (*sat*, *dsrA*), ribosomal proteins of the large (*rplA*) and small subunit (*rpsC*), cell division (*ftsZ*), DNA replication (*gyrB*), and peptidoglycan synthesis (*murA*). Solid lines and symbols represent sulfate-stimulated microcosms whereas dashed lines and open symbols represent control microcosms without external sulfate. Panels represent the various substrate incubations, native stands for native peat soil. Different symbols represent replicates and are consistent throughout all panels.

Fig. 3

Transcription patterns of whole pathways and central enzyme complexes involved in the carbon and energy metabolism of *Desulfosporosinus* MAG SbF1 under *in situ*-like conditions. In addition, transcription patterns of general stress response proteins are shown. Mean abundance for the native soil (—) and each incubation treatment and time point is shown. Supplemented substrates are indicated by initials and addition of external sulfate is depicted by −S/+S (columns). Abundance values are normalized variance-stabilized counts x, which were scaled from 0 to 1 for each CDS using the formula [x – min(x)] / max[x - min(x)]. Incompletely assembled genes are indicated by _a, _b, and _c.

Fig. 1.

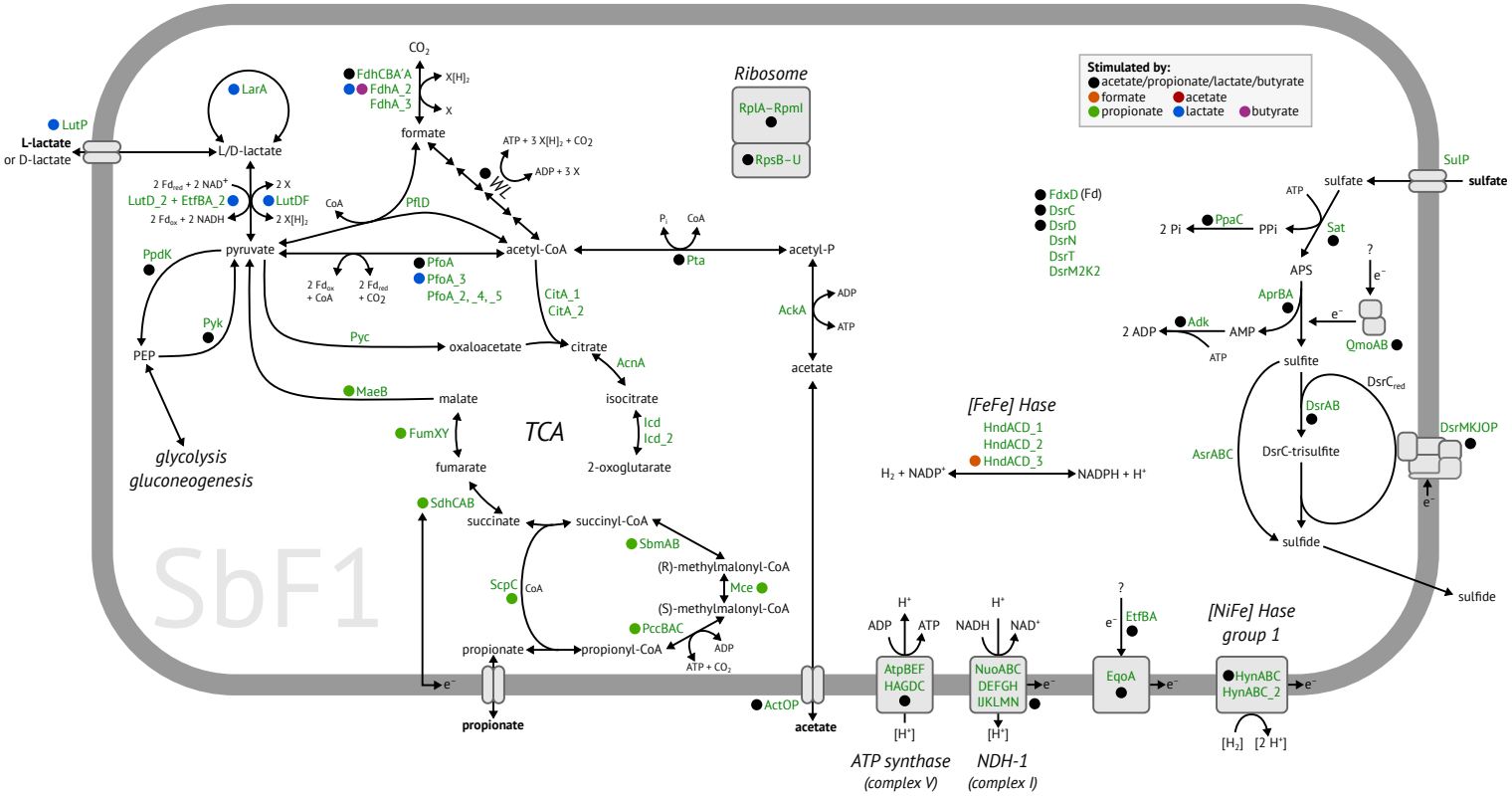

Fig. 2.

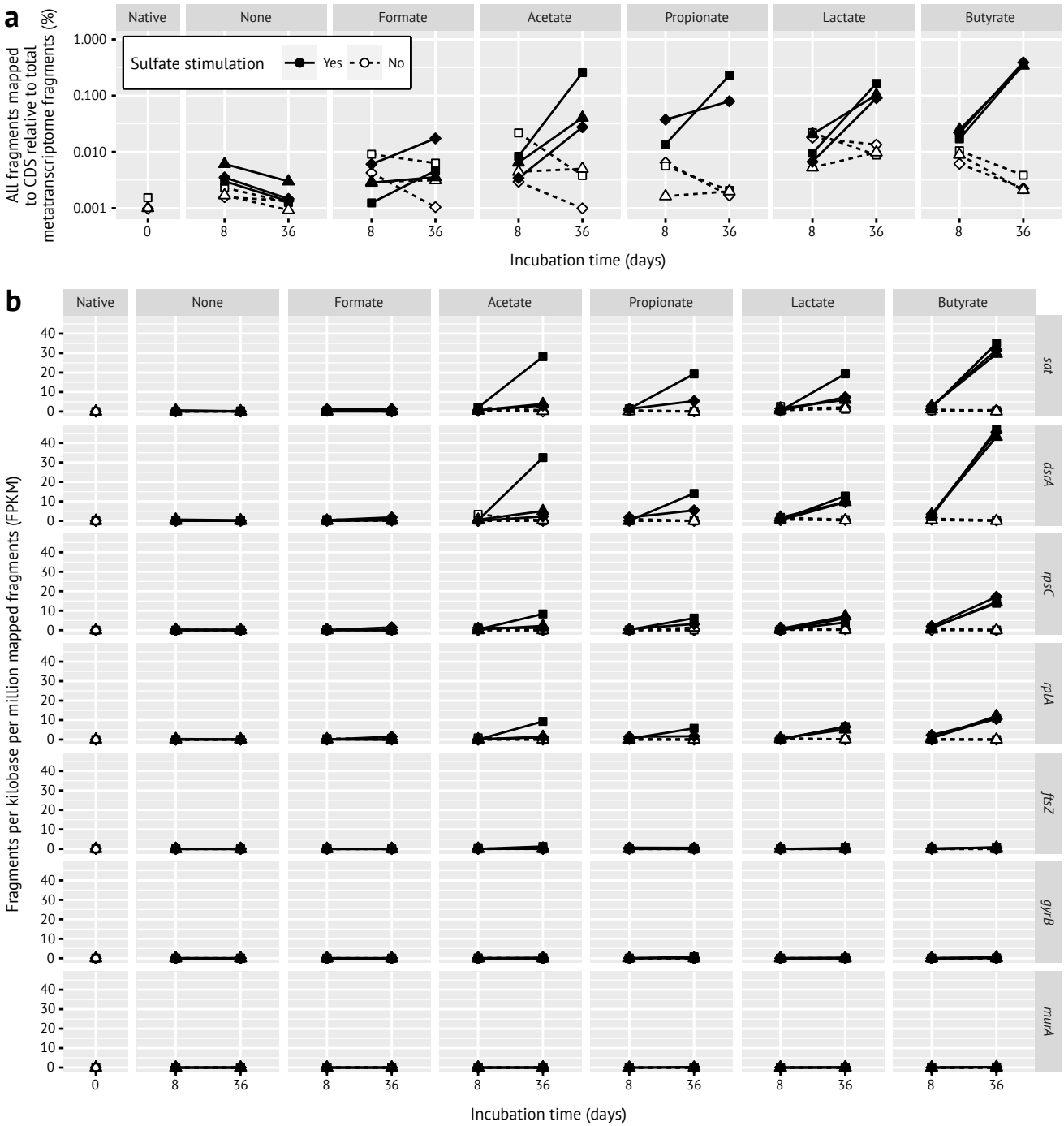

Fig. 3.

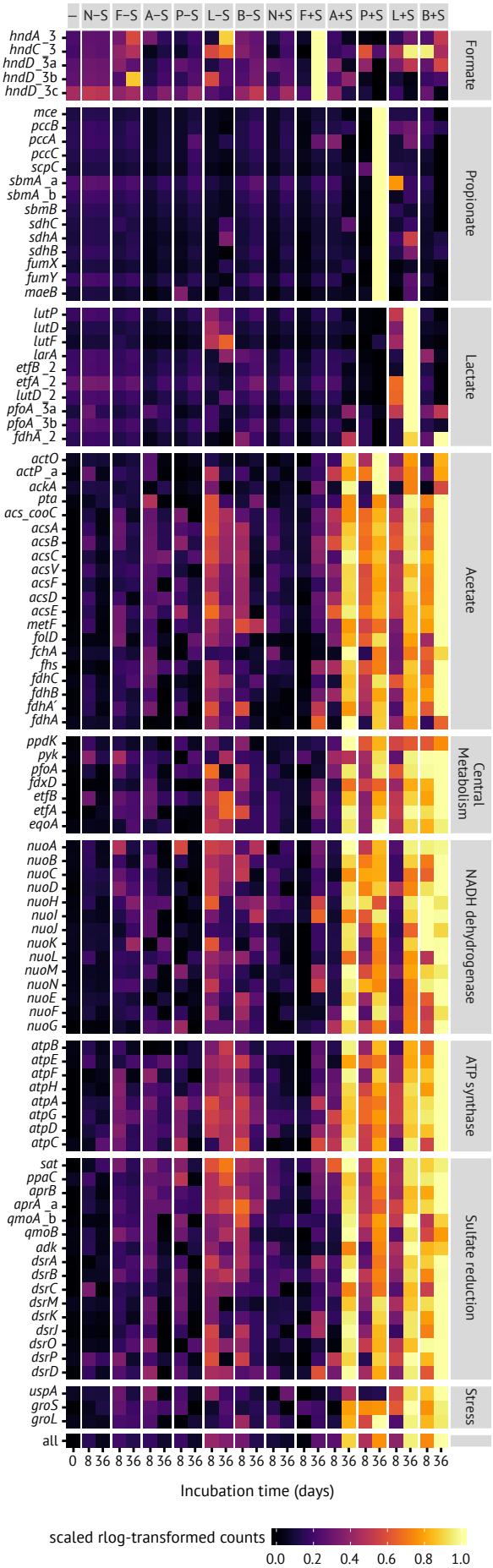

Supplementary Information

Supplementary Tables

Table S1

Summary of all genomic features in *Desulfosporosinus* MAG SbF1. Genes encoding the energy metabolism or central cellular functions are given first. COG class IDs were assigned by MaGe (Cognitor, www.ncbi.nlm.nih.gov/COG/). bactNOG and NOG IDs were assigned by best-match principle (Huerta-Cepas *et al.*, 2016; Hausmann *et al.*, 2018). Spearman's rank correlation is given for each gene's transcripts as compared to total mRNA counts (FDR-adjusted *p*-values are indicated by asterisks: ✱, < 0.05; ✱✱, < 0.01; ✱✱✱, < 0.001). Expression clusters represent the clusters assigned by correlation and hierarchical clustering analysis. The next five columns are $\log_2$ fold-changes of expression levels after 36 days of incubation in the sulfate-stimulated microcosms (i.e., substrate vs no-substrate-control). Missing fold-changes are due to all counts being zero in both compared treatments. Ranks are based on mean fragments per kilobase per million mapped fragments (FPKM). Also here, only data of sulfate-stimulated microcosms after 36 days of incubation are shown in addition to the native soil. Missing ranks indicate that expression was never detected in any replicate. Fragmented, i.e., mainly incompletely assembled genes are indicated by _a, _b, and _c. A ^{1} or ^{2} in the strand column indicates that this CDS is either the first or last on a scaffold, respectively (depending on the reading frame).

Table S2

Characteristics and coverage of all scaffolds belonging to *Desulfosporosinus* MAG SbF1. The two scaffolds with the highest coverage encode the 23S and 16S rRNA genes, respectively.

Table S3

Expression levels of selected CDS in the analysed anoxic peat soil microcosms given in FPKM (mean ± one standard deviation). Loci are sorted as in Table S1. Headers display the individual treatments used in the peat soil microcosms: without and with external sulfate added; amended substrate; and days of incubation.

Supplementary Figures

Fig. S1

Differential coverage plots of assembled scaffolds with *Desulfosporosinus* MAG SbF1 scaffolds highlighted by black circles. The average coverage per scaffold in the SIP metagenome is visualized without (a) and with (b) G+C content transformation (see Materials and Methods). Taxonomic affiliation is indicated by color and based on BLAST as described previously (Albertsen *et al.*, 2013). White circles represent unclassified scaffolds. Only scaffolds >10 000 nt length are shown, except when belonging to SbF1. Scaffolds encoding selected genes in SbF1 are labelled accordingly.

Fig. S2

(a) Maximum likelihood 16S rRNA gene tree of species belonging to the genera *Desulfosporosinus* and *Desulfitobacterium*. Branch supports of ≥0.9 and ≥0.7 are indicated by filled and open circles, respectively. GenBank accession numbers are given in parentheses. (b) Bayesian inference phylogenomic tree showing the phylogenetic placement of *Desulfosporosinus* MAG SbF1. All branches were supported >0.9 (filled circles). The tree was rooted against genomes from the *Acidobacteria*, *Proteobacteria*, and *Verrucomicrobia* (not shown). Genome accession numbers are given in parentheses.

Fig. S3

Two-way average amino and nucleic acid identities between *Desulfosporosinus* and *Desulfitobacterium* species genomes (in%, written into cells). The dendrogram is based on Fig. S2b.

Fig. S4

Time-resolved changes of all unambiguously identified genes related to cell division (a), DNA replication (b) and cell envelope biogenesis (c); *dsrA* is included for reference, analogous to Fig. 2.

Supplementary References

Albertsen M, Hugenholtz P, Skarshewski A, Nielsen KL, Tyson GW, Nielsen PH. (2013). Genome sequences of rare, uncultured bacteria obtained by differential coverage binning of multiple metagenomes. *Nat Biotechnol* **31**: 533–538.

Hausmann B, Pelikan C, Herbold CW, Köstlbacher S, Albertsen M, Eichorst SA *et al.* (2018). Peatland *Acidobacteria* with a dissimilatory sulfur metabolism. *ISME J*. doi:https://doi.org/10.1038/s41396-018-0077-1[10.1038/s41396-018-0077-1].

Huerta-Cepas J, Szklarczyk D, Forslund K, Cook H, Heller D, Walter MC *et al.* (2016). eggNOG 4.5: a hierarchical orthology framework with improved functional annotations for eukaryotic, prokaryotic and viral sequences. *Nucleic Acids Res* **44**: D286–D293.

Fig. S1.

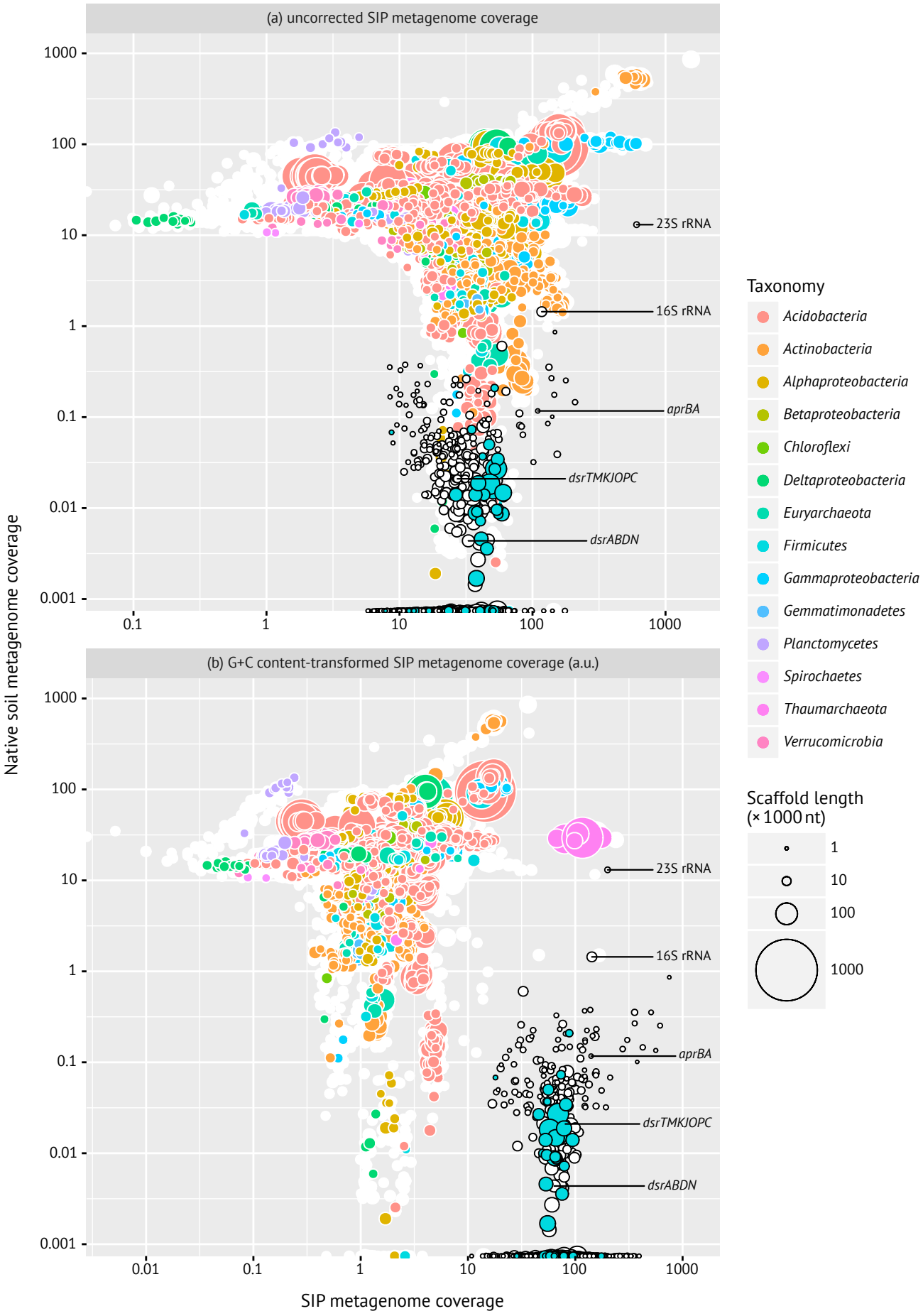

Fig. S2.

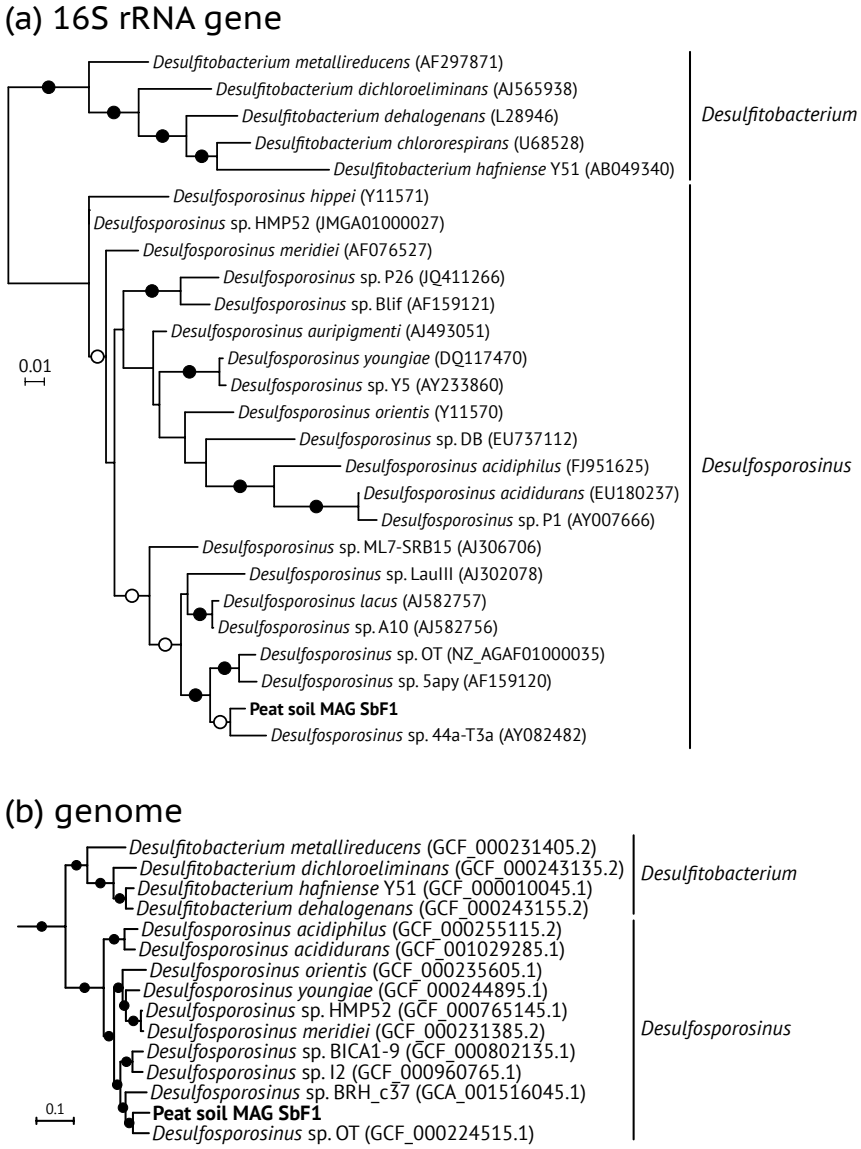

Fig. S5.

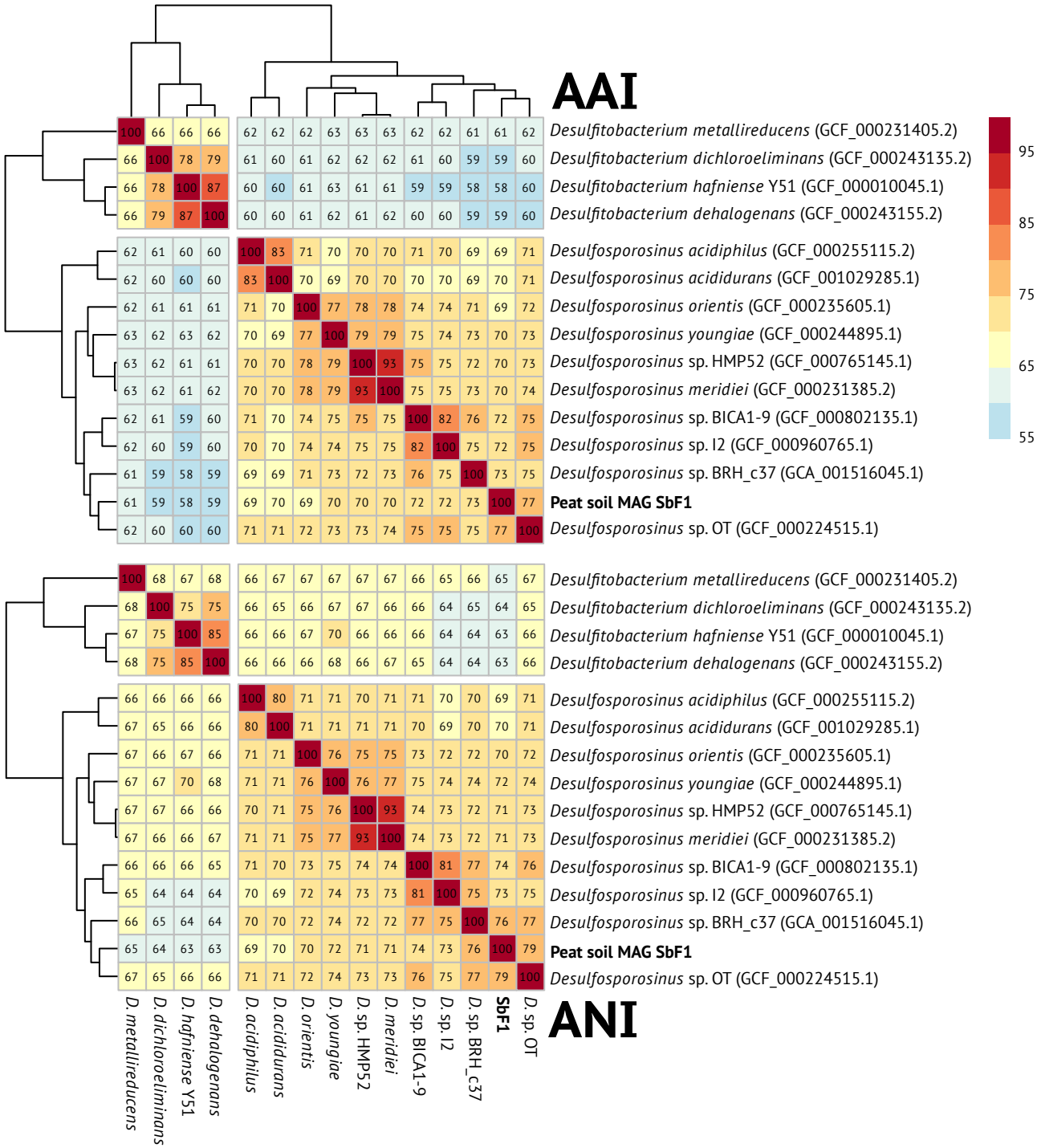

Fig. S4a.

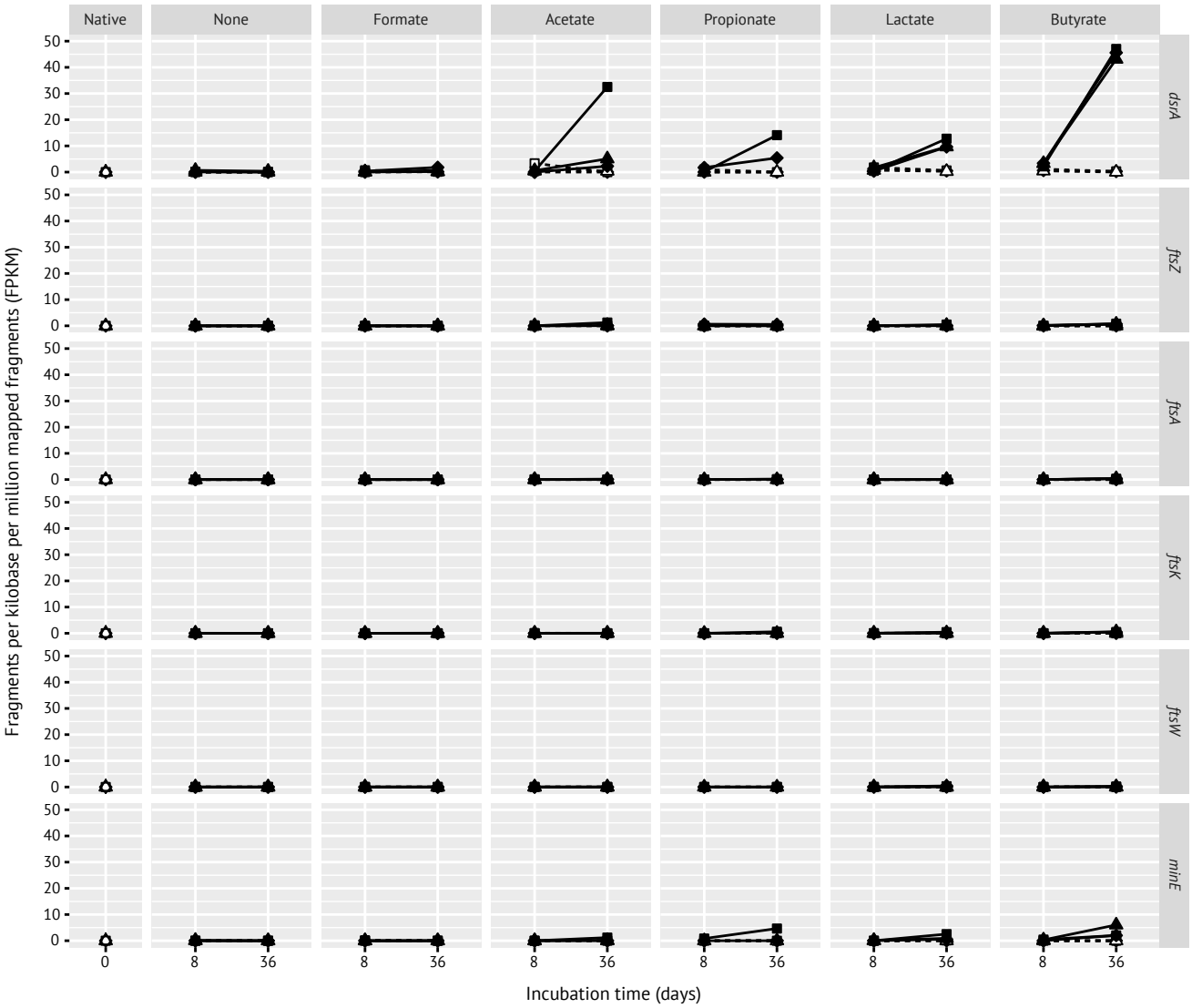

Fig. S4b.

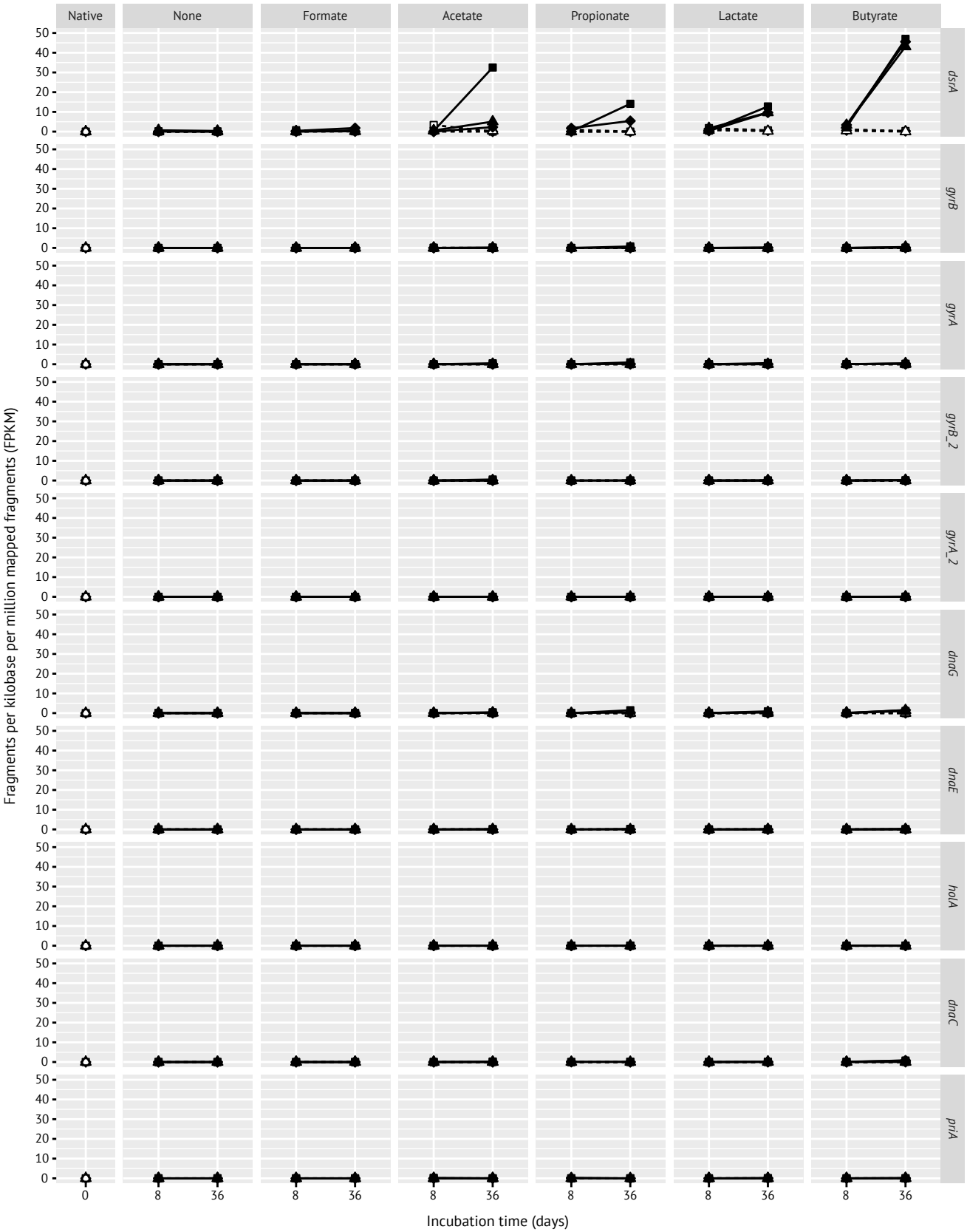

Fig. S4c.